Investigation of electron wave function hybridization in $Ga_{0.25}In_{0.75}As/InP$ arrays

T. P. Martin,[1,2,a)] M. S. Fairbanks,[1,b)] B. C. Scannell,[1] C. A. Marlow,[1] H. Linke,[1,3] and R. P. Taylor[1,4]
[1]*Department of Physics, University of Oregon, Eugene, Oregon 97403, USA*
[2]*School of Physics, University of New South Wales, Sydney 2052, Australia*
[3]*Division of Solid State Physics, Lund University, P.O. Box 118, S-221 00 Lund, Sweden*
[4]*Department of Physics and Astronomy, University of Canterbury, Christchurch 8140, New Zealand*

(Received 14 September 2009; accepted 14 October 2009; published online 5 November 2009)

We present a measurement technique for quantifying coupling between semiconductor quantum dots in an array. This technique employs magnetoconductance fluctuations to probe the decrease in the average spacing of the quantum energy levels as the electron wave functions in the dots undergo hybridization. Focusing on $Ga_{0.25}In_{0.75}As$ dots, we investigate hybridization as the coupling strength is varied and the number of dots in the array is increased. Our technique reveals a significant drop in the average energy level spacing for multiple dot arrays, which is strong evidence for wave function hybridization. © *2009 American Institute of Physics*. [doi:10.1063/1.3258495]

The coupling of quantum electronic devices to form arrays is of considerable interest for both fundamental physics (e.g., quantum coherence[1,2]) and applied physics (e.g., spintronics[2]). From an engineering viewpoint, understanding the interaction of individual devices represents the first step for developing circuits with sophisticated quantum functionality. Whereas the majority of previous coupling studies have focused on electron transport mediated by tunneling between "closed" quantum dots,[1–3] here we focus on the "open" transport regime where the devices are connected by conducting channels.[4–6] We will describe a measurement technique for quantifying the evolution of the quantum energy level spectrum of the open arrays as the coupling strength of the connecting channels is varied and the number of devices in the array, N_{dot}, is increased. This technique employs magnetoconductance fluctuations (MCF) to probe the decrease in the average spacing of the quantum energy levels as the electron wave functions undergo hybridization. Our method is flexible compared to previous spectroscopy techniques, in that it does not require microwave radiation,[1,3] nor is it restricted to probing dots $\lesssim 0.2\ \mu m^2$ in area.[7]

To demonstrate the technique, we investigate arrays of ballistic quantum dots etched into a modulation-doped GaInAs/InP heterostructure,[8] shown schematically in Fig. 1(a). The $Ga_xIn_{1-x}As$ material system is increasingly employed for studies of quantum transport phenomena, such as quantum coherence[9] and engineered conductance asymmetry,[4] rather than the traditional $Al_xGa_{1-x}As/GaAs$ heterostructures.[5,6] The reduced effective mass m^* of our $Ga_{0.25}In_{0.75}As$ quantum well (with a measured $m^*=0.04m_e$ compared to $0.067m_e$ for GaAs) produces larger energy level spacings, making this system optimal for studies of energy level hybridization. Three separate arrays, comprising one, two, and three coupled dots, are defined within a two-dimensional electron gas (2DEG) situated in the 9 nm wide quantum well. The arrays are patterned using electron beam lithography and etched into the mesa of a Hall bar. A uniform Ti/Au electrostatic gate, separated from the heterostructure surface by a 1 μm insulating polymer layer, simultaneously controls the electron density in the Hall bar and in the devices. An electron density, $n_s=6\times10^{11}\ cm^{-2}$, and mean free path, $l_t=3\ \mu m$, are obtained at a top gate bias of $V_g=0$ V and temperature $T=240$ mK. Further details of the heterostructure can be found in the literature.[8,10]

The two and three dot arrays are shown in the scanning electron microscopy (SEM) images of Fig. 1(b). These and the one dot array are defined in the same Hall bar to ensure an identical material environment. Each component dot has

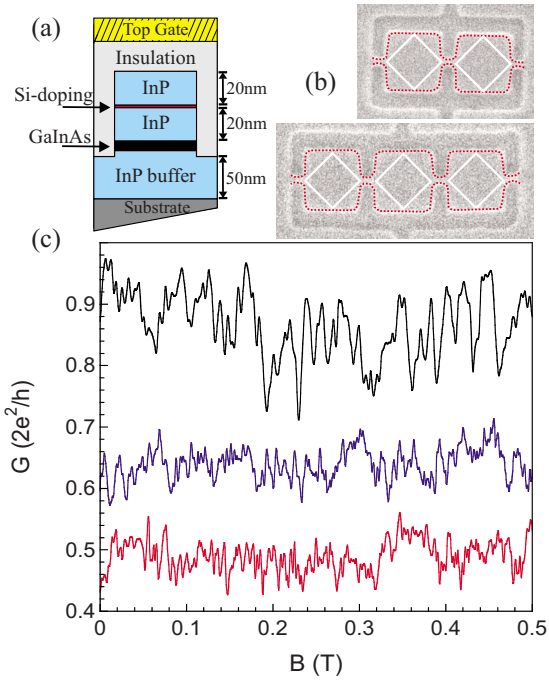

FIG. 1. (Color online) (a) The $Ga_{0.25}In_{0.75}As/InP$ heterostructure etched to a narrow channel, (b) an SEM image of the double and triple dot arrays with a typical depletion profile (dotted) and the smallest enclosed electron trajectories, (c) MCF for the single, double, and triple dot arrays (top to bottom) at $N_{1,2}\approx1$. MCF for the single dot are offset $0.2\times(2e^2/h)$ for clarity.

a)Current address: Naval Research Laboratory, Washington, DC 20375.
b)Electronic mail: mfairban@uoregon.edu.

 © 2009 American Institute of Physics

Downloaded 05 Nov 2009 to 128.223.130.212. Redistribution subject to AIP license or copyright; see http://apl.aip.org/apl/copyright.jsp

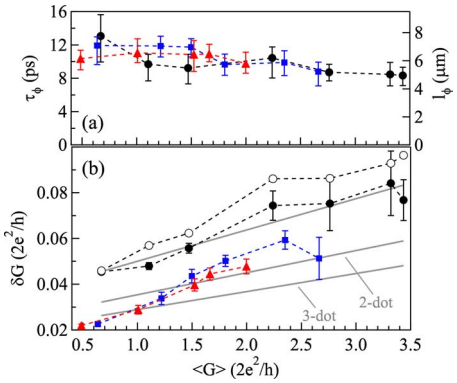

FIG. 2. (Color online) (a) Phase coherence time τ_ϕ and length l_ϕ vs coupling strength, $\langle G\rangle$, for the single (circles), double (squares), and triple (triangles) dot arrays. (b) RMS amplitude of the conductance δG vs $\langle G\rangle$ for the three arrays. Open circles are a theoretical prediction for the single dot based on random matrix theory. The solid lines are a linear fit to the data for the single dot, and the same fit scaled by $1/\sqrt{2}$ and $1/\sqrt{3}$ assuming ensemble averaging (see text).

a square geometry with lithographic dimensions of 0.77 $\times 0.73$ μm^2 (± 0.01 μm). The dots are smaller than the mean free path to ensure that conduction within a dot is ballistic. Each dot is coupled to its neighbors by nominally identical quantum point contacts (QPCs) with lithographic widths of 100 ± 5 nm. Typical electrostatic depletions are shown in Fig. 1(b). The etched confinement potential in these devices is an order of magnitude steeper than the equivalent in surface gate-defined devices,[10] which enables the number of conducting channels in the QPCs to be altered by the top gate without significantly perturbing the dot geometry.

The arrays were cooled to $T=240$ mK in a ^{3}He refrigerator and their conductance G was measured using lock-in detection (37 Hz) methods in a four-probe configuration at a 1 nA constant current. The MCF were measured at plateaus observed in the conductance of each array versus V_g, Fig. 1(c) shows the MCF measured on the first plateau. We parameterize coupling between dots within each array using the mean conductance $\langle G\rangle$ of the MCF, which increases as the gate populates additional modes in the QPCs. The mean was taken at magnetic fields (B) where chaotic transport and time-reversal symmetry breaking occur simultaneously ($0.02\ \text{T} < B < 0.4\ \text{T}$).[9] The MCF at these fields can be analyzed using random matrix theory (RMT),[9,11,12] which plays an important role in our technique.

Since the MCF are generated by quantum interference of phase coherent electrons, the electron phase coherence time τ_ϕ is a crucial parameter. We use an established method to measure τ_ϕ based on the correlation field (B_c) at magnetic fields sufficiently large ($B > 0.5$ T) that electron conduction occurs in the skipping-orbit regime.[13] Figure 2(a) shows τ_ϕ and the equivalent phase-breaking length l_ϕ for each array ($l_\phi = v_F \tau_\phi$, where v_F is the electron Fermi velocity) plotted as a function of $\langle G\rangle$. As expected for identical material environments, all three arrays reveal approximately the same phase coherence length of $l_\phi \approx 6$ μm. This value decreases slightly as the number of coupling modes N increases. This suppression has been explained in terms of the increased exposure of the dots to the 2DEG environment.[14]

We begin our investigation of the energy level spectrum by considering the single dot device. The average energy level spacing ΔE_S is determined by combining two previously established methods for extracting τ_ϕ from the MCF: the correlation field analysis discussed above[13] and an analysis of the average amplitude of the low-field MCF, δG. In this second method, δG can be related to fundamental device parameters via a conductance correlation function derived from RMT,[9,12]

$$(\delta G)^2 = \int_0^\infty \int_0^\infty f'(E) f'(E') \times \frac{\langle G\rangle^2}{(N+N_\phi)^2 + 4\pi^2 (E-E')^2/\Delta E_S^2} dE dE', \qquad (1)$$

where $N = N_1 + N_2$ is the total number of modes in the entering and exiting QPCs and $f'(E)$ is the derivative of the Fermi function. In this model, suppression of phase coherence is analogous to electrons escaping the dot through a fictitious lead attached to a phase-randomizing reservoir. The escape rate is set by ΔE_S and is related to N_ϕ by the expression $N_\phi = 2\pi\hbar/\tau_\phi \Delta E_S$.[15]

Figure 2(b) shows δG plotted as a function of $\langle G\rangle$ for the three arrays. Figure 2(b) also includes a calculation of $\delta G = N_1 N_2/(N^2 + N_\phi N)$ for the single dot based on a zero-temperature RMT prediction that includes phase decoherence.[11] For this theory, the number of physical modes in the QPCs are calculated from the mean conductance $\langle G\rangle = [1/N_1 + 1/N_2]^{-1}$ $(2e^2/h)$,[11] while $N_\phi = m^* A/\hbar\tau_\phi$ is calculated using the dot's enclosed area A obtained from simulations of the confinement potential.[10] The observed reduction in the measured values of δG compared to this theory is expected due to the suppression of the MCF amplitude at finite temperature. The close agreement between the measured and predicted trends in δG for the single dot confirms the applicability of RMT to these devices.

Previous research has shown that values of τ_ϕ obtained from Eq. (1) and those extracted from the correlation field analysis are consistent.[9] Thus we propose extracting ΔE_S from Eq. (1) by numerical integration, using the values of τ_ϕ from the correlation analysis along with the measured values for N, δG, T, and $\langle G\rangle$. The results of this method are shown in Fig. 3(a). For comparison, we have included the value of ΔE_S calculated from the dot's enclosed area A. This simple approximation shows a downward trend with $\langle G\rangle$ caused by the increase in A due to decreased electrostatic depletion. Values of ΔE_S measured using Eq. (1) show an even steeper decrease, which we assign to a combination of reduction in area and also an increase in hybridization between the wave functions in the dot and QPCs.

We can now apply the technique to investigate the coupling between dots in the double and triple arrays. Figure 1(c) compares the MCF for the three arrays measured at the first conductance plateau ($N_1, N_2 \approx 1$). By inspection, the MCF show: (1) a decrease in δG as the number of dots in the arrays increase and (2) an increase in high frequency content in the double and triple dot arrays. To explain these observations, we first consider the possible scenario that each dot in an array acts as an isolated quantum system, i.e., the wave functions do not couple, but are instead spatially contained within the square geometry of the dot. If this is the case, then the MCF generated by each dot in the array will be independent of the MCF from neighboring dots. This will lead to ensemble averaging of the MCF, such that δG_{total}

Downloaded 05 Nov 2009 to 128.223.130.212. Redistribution subject to AIP license or copyright; see http://apl.aip.org/apl/copyright.jsp

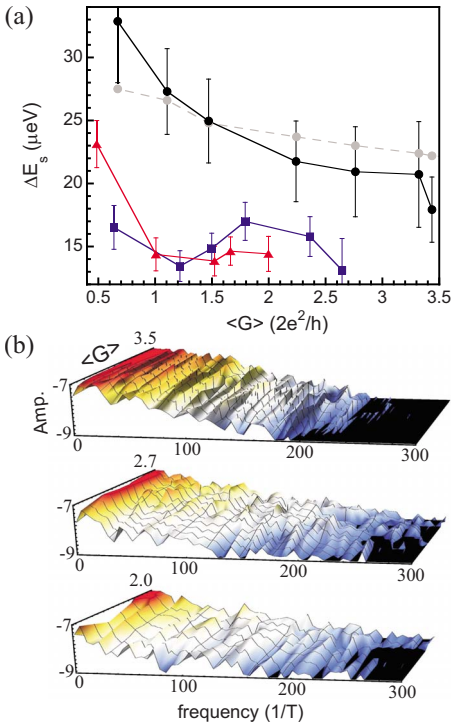

FIG. 3. (Color online) (a) Average energy level spacing ΔE_S for the single, double, and triple dot arrays (black circles, squares, and triangles, respectively). An estimate of ΔE_S based on lithographic area and depletion measurements (gray circles) is shown as a baseline for the single dot. (b) Fourier spectra for the three arrays (1–3 dots from top to bottom) that share common frequency and (logarithmic) Fourier amplitude axes. The maxima in $\langle G \rangle$ are indicated on the *y*-axis for each array.

$= \delta G_{\mathrm{dot}} / \sqrt{N_{\mathrm{dot}}}$. The solid gray lines in Fig. 2(b) plot the trend in δG for the single dot and for a double and triple array assuming ensemble averaging. These trends do not fit to the measured data for the double and triple arrays, indicating that wave function coupling must be occurring between the dots. The absence of ensemble averaging has also been observed for open dot arrays in GaAs heterostructures.[14]

Our technique for evaluating ΔE_S can be used to quantify the extent of this coupling. Figure 3(a) shows a significant drop in ΔE_S between the single and double dot arrays, which is consistent with hybridization of the double array's energy spectrum. Intriguingly, the triple dot array shows a degree of hybridization similar to the double array. This can be understood by examining the characteristic l_ϕ values in Fig. 2(a). Picturing the smallest quantum interference loop as the diamond shapes shown in Fig. 1(b), the minimum perimeter for a loop spanning the double array is 4.2 μm, while for the triple array it is 6.4 μm. Thus the measured $l_\phi \simeq 6$ μm easily accommodates the minimum perimeter coherent interference loop spanning the double array, but the corresponding loop perimeter in the triple array is $\gtrsim l_\phi$ and has a much reduced likelihood of coherent transport over all three dots.

The limited phase coherence in the triple array is further substantiated by inspection of the Fourier spectra in Fig. 3(b). Higher frequency fluctuations correspond to a larger spatial extent of electron quantum interference loops,[16] which we would expect for larger coherent systems like the hybridized arrays.[6] The double dot array has significantly more high frequency content than the single dot. However, the triple dot array shows no appreciable difference compared to the double array, confirming that the extent of hybridization is limited by de-phasing in the third dot. We note that the mild downward trend in ΔE_S observed in Fig. 3(a) for the three devices is reflected in the Fourier spectra, with higher frequency structure increasing mildly with coupling strength $\langle G \rangle$.

In summary, we have demonstrated a quantitative method for extracting ΔE_S, which is a direct indicator of wave function hybridization in an array of ballistic quantum dots. Our arrays showed hybridization over the entire range of measured coupling strengths ($N_{1,2} \approx 1-4$). Future devices will benefit from smaller component dots and/or improved materials, which will permit coherent transport over more complicated geometries. We note that, although this letter concentrated on ballistic transport, the τ_ϕ measurement methods that formed the basis of our measurement technique have analogous expressions for the diffusive transport regime.[17] Thus the technique explored here could be expanded to act as a generic tool across a wide range of coupled quantum devices.

We acknowledge support from the AFRL (Agreement No. FA8650-05-1-5041), the ONR through the Oregon Nanoscience and Microtechnologies Institute, the Swedish Research Council, and the NSF IGERT program (M.S.F. and T.P.M.). R.P.T. is a Cottrell Scholar of the Research Corporation.

[1] R. H. Blick, D. Pfannkuche, R. J. Haug, K. v. Klitzing, and K. Eberl, Phys. Rev. Lett. **80**, 4032 (1998).
[2] E. A. Laird, J. R. Petta, A. C. Johnson, C. M. Marcus, A. Yacoby, M. P. Hanson, and A. C. Gossard, Phys. Rev. Lett. **97**, 056801 (2006).
[3] T. H. Oosterkamp, T. Fujisawa, W. G. van der Wiel, K. Ishibashi, R. V. Hijman, S. Tarucha, and L. P. Kouwenhoven, Nature (London) **395**, 873 (1998).
[4] C. A. Marlow, R. P. Taylor, M. Fairbanks, I. Shorubalko, and H. Linke, Phys. Rev. Lett. **96**, 116801 (2006).
[5] M. Elhassan, J. P. Bird, A. Shailos, C. Prasad, R. Akis, D. K. Ferry, Y. Takagaki, L.-H. Lin, N. Aoki, Y. Ochiai, K. Ishibashi, and Y. Aoyagi, Phys. Rev. B **64**, 085325 (2001).
[6] N. Aoki, D. Oonishi, Y. Iwase, Y. Ochiai, K. Ishibashi, Y. Aoyagi, and J. P. Bird, Appl. Phys. Lett. **80**, 2970 (2002).
[7] I. V. Zozoulenko, A. S. Sachrajda, C. Gould, K.-F. Berggren, P. Zawadski, Y. Feng, and Z. Wasilewski, Phys. Rev. Lett. **83**, 1838 (1999).
[8] P. Ramvall, N. Carlsson, I. Maximov, P. Omling, L. Samuelson, W. Seifert, Q. Wang, and S. Lourdudoss, Appl. Phys. Lett. **71**, 918 (1997).
[9] B. Hackens, S. Faniel, C. Gustin, X. Wallart, S. Bollaert, A. Cappy, and V. Bayot, Phys. Rev. Lett. **94**, 146802 (2005).
[10] T. P. Martin, C. A. Marlow, L. Samuelson, A. R. Hamilton, H. Linke, and R. P. Taylor, Phys. Rev. B **77**, 155309 (2008).
[11] P. W. Brouwer and C. W. J. Beenakker, Phys. Rev. B **55**, 4695 (1997).
[12] P. W. Brouwer, J. N. H. J. Cremers, and B. I. Halperin, Phys. Rev. B **65**, 081302 (2002).
[13] J. P. Bird, K. Ishibashi, D. K. Ferry, Y. Ochiai, Y. Aoyagi, and T. Sugano, Phys. Rev. B **51**, 18037 (1995).
[14] M. Elhassan, J. P. Bird, R. Akis, D. K. Ferry, T. Ida, and K. Ishibashi, J. Phys.: Condens. Matter **17**, L351 (2005).
[15] C. M. Marcus, R. M. Westervelt, P. F. Hopkins, and A. C. Gossard, Phys. Rev. B **48**, 2460 (1993).
[16] R. P. Taylor, M. L. Leadbeater, G. P. Whittington, P. C. Main, L. Eaves, S. P. Beaumont, I. McIntyre, S. Thoms, and C. D. W. Wilkinson, Surf. Sci. **196**, 52 (1988).
[17] C. W. J. Beenakker, Rev. Mod. Phys. **69**, 731 (1997).

Downloaded 05 Nov 2009 to 128.223.130.212. Redistribution subject to AIP license or copyright; see http://apl.aip.org/apl/copyright.jsp